Health Environ, 2025, 6(1): 281-293
DOI: 10.25082/HE.2025.01.001

RESEARCH ARTICLE

# Oil Spill Cleanup with Raw *Luffa Aegyptiaca* Sponge: Modification Effects, Sorption Isotherm, Kinetics and Thermodynamics

**Adaku Chinonyerem Ajiwe**[1*] **Patrice-Anthony Chudi Okoye**[1] **Uche Eunice Ekpunobi**[1]

[1] Department of Pure and Industrial Chemistry, Nnamdi Azikiwe University, Awka, Anambra, Nigeria

Check for updates

**Correspondence to:** Adaku Chinonyerem Ajiwe, Department of Pure and Industrial Chemistry, Nnamdi Azikiwe University, Awka, Anambra, Nigeria;
E-mail: aajiwe@yahoo.com

**Received:** June 9, 2025;
**Accepted:** September 18, 2025;
**Published:** September 25, 2025.

**Citation:** Ajiwe AC, Okoye PAC, Ekpunobi UE. Oil Spill Cleanup with Raw *Luffa Aegyptiaca* Sponge: Modification Effects, Sorption Isotherm, Kinetics and Thermodynamics. *Health Environ*, 2025, **6**(1): 281-293. https://doi.org/10.25082/HE.2025.01.001

**Copyright:** © 2025 Ajiwe AC *et al*. This is an open access article distributed under the terms of the Creative Commons Attribution-Noncommercial 4.0 International License, which permits all non-commercial use, distribution, and reproduction in any medium, provided the original author and source are credited.

**Abstract:** Oil spill can be extremely hazardous and environmentally threatening, and therefore needs to be contained and cleaned up as soon as possible. These serious environmental consequences have long been recognized and considerable research and technological development has been carried out to develop appropriate remediation techniques. Most of the sorbents in use for cleanup technologies are synthetic, non-biodegradable and imported. There is need to develop natural sorbents which are biodegradable, cost effective and readily available in line with agricultural wastes *Luffa aegyptiaca* sponge were functionalized by acetylation to increase their hydrophobic properties and oil sorption capacities. Structural modification from acetylation of *Luffa aegyptiaca* sponge was analyzed using Fourier Transform Infrared Spectroscopy (FTIR). The effect of time and catalysts (KBr and KI) on the acetylation process was examined to optimize conditions. Sorption behaviours was studied using kinetic models, including first, Hill second, Pseudo-second and Intra-particle diffusion models. Isotherm models such as Langmuir, Freundlich and Temkin isotherm model were also used to analyze the crude oil sorption behaviour. The results reveal that the acetylation significantly enhanced the hydrophobic properties of the materials. The kinetic studies of all the samples demonstrated that acetylation process adhered to pseudo-second order kinetics model with high $R^2$ values. In the crude oil sorption analysis, the values of the coefficient of determination indicated that the Freundlich isotherm model has a better correlation, by implying that the adsorption from acetylation is heterogeneous and multi-layered. The FTIR spectra confirmed successful acetylation through the presence of characteristic functional groups. The SEM analysis of the acetylated sample revealed significant changes in surface morphology, with increased porosity and roughness compared to the raw samples. The findings demonstrated that the acetylated materials could serve as effective, natural sorbents for oil spill remediation, offering a sustainable and cost effective alternatives to synthetic sorbents.

**Keywords:** *Luffa aegyptiaca*, acetylation, oil spillage, crude oil sorption

## 1 Introduction

The potential of many low coat adsorbents for the removal of oil spill have been investigated by many researchers. These wastes are locally available, inexpensive and biodegradable which has made researchers study them as alternatives to the imported synthetic sorbent materials which are expensive and non-biodegradable. These low cost adsorbents include agricultural by-products and waste materials, fly ash, seaweeds and alginate, peat moss, biomass materials and many others. The acetylation of corn silk and its application for oil sorption was reported by Asadpour et al. (2015) [1]. The acetylation was done with acetic anhydride using N-Bromosuccinimide catalyst. The effect of contact time, concentration of catalyst and temperature were studied. The result showed that the highest oil sorption was 11.45% weight percent gain (WPG) and was achieved at 3% catalyst concentration in acetic anhydride and temperature of 120$^o$C for 6 hours. They observed that the sorption capacity of Tapis and Arabian crude oil using corn silk was 8.6 and 9.4 g/g respectively. It was found that the best condition for acetylation was 3 % catalyst for 6-hour reflux at 120$^o$C which showed maximum WPG and oil sorption capacity of 14.02 and 16.88g/g, and optimum contact time of 30 and 40 minutes for Tapis and Arabian crude oil respectively. The characteristics of raw and acetylated corn silk were examined using FTIR and SEM and the treated corn silk was found to have higher sorption capacity than that of the raw sample. El-Din et al. (2018) [2], analyzed the oil sorption capacity

of banana peel from local fruit wastes. The research showed that the surface properties, oil type, oil film thickness, sorption time, temperature and salinity all affect sorption capacity. It was observed that the best condition for sorption was at an average particle size of 0.3625 mm at 25$^o$C, 15 minutes sorbent time, 3.5% artificial seawater and 5mm oil thickness. They noted that the sorbent can be reused more than 10 times to reach 50% of the first sorption value. It was concluded that the sorption capacity of banana peel gave a good result as a new and low cost agriculture waste for oil clean up. The use of a by-product of peat excavation and cotton grass fibre as a sorbent for oil spills was investigated by Sun et al. (2004) [3]. They observed that cotton grass fibre has absorbed oil approximately two to three times as much, and two to three times as fast as the synthetic one. In removing diesel oil from the surface of water, the efficiency was over 99% up to an absorbing factor of 20 times its own weight. The biodegradable cotton grass fibre proved to be effective oil sorbent with raw – material cost. Ola et al. (2017) [4], investigated the efficiency of raw and modified palm fibers as adsorbent for different oils. Their result revealed that the adsorption capacity of the fibers was found to increase with time, thickness of oil film, temperature and particle size while it decreases with mass of adsorbent, they described the adsorption process as monolayer coverage and the maximum adsorption capacity of palm fibers was found to be 35.71, 22.73 and 21.74g oil/g adsorbent for diesel, crude and vegetable oil respectively. Reza et al. (2013) [5], studied the application of *Phragmites australis*, sugarcane leaves straw and sugarcane bagasse for crude oil sorption in dry (only oil) systems. The results indicated that sugar cane bagasse had a higher oil sorption capacity compared to the other due to its higher porosity and lower density. The effect of sorbent contact time and its particle size on oil adsorption capacity were evaluated for the systems of dry and crude oil layer on water. The results showed that the maximum adsorption capacity of raw sugarcane bagasse for dry system and crude oil layer system was about 8 and 6.6g/g respectively. It was also observed that most oil was adsorbed at the early stage of the process (within a few minutes) and, afterwards, a small amount of oil will be adsorbed. Nurul et al. (2011) [6], studied the sorption equilibrium and kinetics of oil sorption using banana pseudo-stem fibers (BP) in Malaysia. It was observed to be an efficient sorbent for the removal of oil in water and it may be an alternative to costlier adsorbents such as activated carbon. The studies clearly suggest that BP exhibits almost 100% adsorption at lower concentration of oil. Equilibrium data fitted well with the Freundlich model, which suggests a coverage of oil molecules on the surface of BP. The kinetic data were best fitted to a pseudo second-order kinetic model. The effect of Kapok fiber treated with various solvents on oil absorbency was investigated by Jintao et al. (2012) [7]. The fiber was treated with various solvents like water, HCl, NaOH, $NaClO_2$and chloroform to improve the efficiency for oil absorbency the structure of untreated and treated Kapok fiber was investigated and compared using FTIR, SEM and XRD. The effects of treatment concentration, temperature and time on oil absorbency were assessed with toluene, chloroform, n-hexane and xylene as the model oils. The results indicated that except for chloroform, Kapok fibers treated with other solvents show enhanced oil absorbency, with increase in percentage found to be 19.88%, 30.0%, 21.55% for toluene, chloroform, n-hexane and xylene respectively. In addition, the solvent-treated Kapok fiber exhibits better re-useability, suggesting its great potential for oil recovery. Rotar et al. (2014) [8], reviewed the efficiency of using natural sorbent materials for cleanup of water surface from oil spills. The oil capacity, buoyancy, solubility of hydrocarbons water and water absorption were the indicators used to compare sorption efficiency determined that the peat moss carbonized at the temperature of 200 – 250$^o$C and modified by acetic acid has high sorption capacity. Also the sorbent increased the efficiency of water surface cleaning up until the water was almost clean and the residual oil content in water was less than 0.03g/L. As the calcification degree of the sorbent increased, its technical application characteristics improved. It was observed that the sorbents were porous with rather developed cell structure allowing them to absorb the products well and retain them for a long time. Acetylation of raw cotton for oil spill cleanup application was investigated by Adebajo and Frost (2004) [9].

# 2 Material and Methods

## 2.1 Materials

*Luffa aegyptiaca* (Igbo name: sponge gourd (wild vegetable sponge), were obtained from Luffa trees in the Aba Abia state environment of Abia state, Nigeria. The mature seeds were collected after the fruits fell off the trees. Each seed was cracked open manually and deseeded. The husks were washed with clean water, dried under the room temperature for 24 hours, then left to dry in the oven at 30$^o$C until constant weight was attained. The dried sponges were ground using a manual grinding machine and sieved. The portions that passed through size

25 British standard sieves and retained by size 36 were used for further analysis. Figure 1 shows digital images of the unmodified *Cucurbita moschata* seed. The crude oil samples were collected from Nigeria National Petroleum Corporation (NNPC) Port-Harcourt Nigeria


**Figure 1** Digital image of (a) native, (b) pilled *Luffa aegyptiaca* sponge and (c) Luffa aegyptiaca pod

## 2.2 Methods

### 2.2.1 Acetylation of the unmodified *Luffa aegyptiaca* sponge

The acetylation of the samples under mild conditions, in the presence of KBr and KI catalyst, using acetic anhydride was carried out using the method of Sun et al. (2004) [3]. The amount of substrate and reactant were combined in a ratio of 1:20. The reaction temperature was 30$^{o}$C, time was differently varied from 30 minutes to 240 minutes at 30 minutes intervals and the catalyst concentration varied from 0.2 g to 1.6 g at 0.2 g interval. The mixture of the raw sorbents, acetic anhydride and catalyst was placed in a round bottom flask fitted to a condenser. The flask was placed in an oil bath on top of a thermostatic heating device, thereafter, the flask was removed from the bath and the hot reagent was decanted off. The sorbents were thoroughly washed with ethanol and acetone to remove un-reacted acetic anhydride and acetic acid as by-products. The new products were dried in an oven at 60$^{o}$C for 16 hours prior to analysis. The degree acetylation was estimated from the infrared spectra by calculating the ratio (R) between the intensity of the acetyl C=O stretching band 1740 - 1745cm$^{-1}$ and the intensity of the C-O stretching vibrations of cellulose backbone at about 1020-1040 cm$^{-1}$ as shown below [9].

### 2.2.2 Effect of acetylation duration

To determine the effect of acetylation duration on the samples, the acetylation reaction was allowed to take place for 30, 60, 90, 120, 150, 180 and 240 minutes using different samples and the degree of acetylation was estimated for the various durations. The data from this analysis were used for kinetic study of the acetylation processes.

### 2.2.3 Effects of catalyst concentration

To determine the effect of catalyst concentration on the samples 0.200 to 0.206g of the catalyst were used at room temperature. The degree of acetylation was estimated for the various catalyst concentrations after 1 hour of reaction.

### 2.2.4 Effect of contact time

To determine the effect of contact time on the crude oil adsorption behaviour of the adsorbents, samples were taken from the adsorption system after 1, 3, 5, 10 and 15 minutes of contact. The amount of crude oil adsorbed, as well as the sorption capacity of the adsorbents at each time interval were determined. The data from this analysis were used for kinetic and mechanism study of the adsorption processes.

## 2.3 Characterization of Adsorbents

The topographical and morphological information about the sample were provided by SEM through the high-resolution, three dimensional and high depth-of-field images of the sample surface and near-surface. The surface morphologies of the raw and acetylated adsorbents were observed with a scanning electron microscope using the method reported by Mohammed and Abdullah (2019) [10]. About 20 mg of the oven–dried samples were mounted on a metallic stub

with a conductive carbon tape and coated with a thin layer of carbon to form a conductive layer around the sample and to prevent accumulation of electron beams. Micrographs of the samples were obtained after irradiation with a 20kv beam of electrons under vacuum. It revealed spatial variations in chemical compositions of the samples and their porous natures.

## 2.4 Crude Oil Sorption

In order to simulate the oil spill situation and to minimize experimental variation, the crude oil was held in a beaker for one day in open air to release volatile hydrocarbon contents. The sorption of oil from water was carried out using batch method as reported by Nwadiogbu et al. (2016) [11]. A portion 0.2 g of each of the raw and acetylated adsorbents was placed in a 250 mL beaker containing 10 g of the weathered crude oil displaced in 100 mL of water at 26$^o$C. The samples were left in the mixture for 15 minutes with little agitation. The sorbents were then removed from the beakers using sieving nets. Then the oil-loaded sorbents were dried at 60$^o$C for 30 minutes and re-weighed. The oil sorption capacity was calculated according to the standard method [12] as shown in equation 3.14 [13].

$$\text{Oil sorption capacity (g/g)} = \frac{W_1 - W_0}{W_0} \quad (1)$$

Where $W_0$ and $W_1$ are the weight of adsorbent before and after oil absorption, respectively and the quantity $W_1 - W_0$ is the amount of crude oil adsorbed in grams. The amount of crude oil adsorbed per unit weight of adsorbent, $q_e$ (mg/g) was calculated using equation 2.

$$q_e = \frac{(C_0 - C_e)V}{m} \quad (2)$$

Where, $C_0$ is the initial crude oil concentration (mg/L), $C_s$ is the equilibrium crude oil concentration (mg/L), V is the volume of the solution (L), and m is the mass of the adsorbent (g).

The effect of the adsorbent dose on the crude oil sorption behaviour of the adsorbents was also studied using weight size from 0.2, to 1.0 g of each adsorbent for a sorption duration of 5 minutes. The sorption processes were also performed using 50, 75, 100, 125, and 150 g/L of crude oil with 0.2g adsorbent for 5 minutes. Data obtained were used for equilibrium studies of the adsorption processes using the isotherm models stated in Table 1. The effect of contact time on the oil sorption behaviours of the adsorbents wasted by carrying out the sorption experiments for a duration of 5, 10, and 15 minutes. The kinetic models presented in Table 2 were used to investigate the sorption kinetics. Additionally, the sorption processes were performed at 30$^o$C, at operating conditions of 100 g/L crude oil, 0.2 g adsorbent, 5 minutes to determine the effect of time on the sorption capacity of the adsorbents and for thermodynamic studies of the adsorption processes.

**Table 1** Selected isotherm models investigated

| SN | Type | Linear form | Plot | Parameters | Reference(s) |
|---|---|---|---|---|---|
| 1 | Freundlich model | $\ln q_e = \ln K_F + \frac{1}{n}\ln C_e$ | $\ln q_e$ vs $\ln C_e$ | Slope = $\frac{1}{n}$; Intercept = $\ln K_F$ | [14] |
| 2 | Temkin | $q_e = B\ln A + B\ln C_e$ | $q_e$ vs $\ln C_e$ | Slope = B; Intercept = B$\ln A$ | [15] |
| 3 | Langmuir | $\frac{C_e}{q_e} = \frac{1}{K_L q_m} + \frac{C_e}{q_m}$ | $\frac{C_e}{q_e}$ vs $C_e$ | Slope = $\frac{1}{q_m}$; Intercept = $\frac{1}{K_L q_m}$ | [16] |

**Table 2** Selected kinetic models investigated

| SN | Type | Linear form | Plot | Parameters | Reference(s) |
|---|---|---|---|---|---|
| 1 | First-order Kinetics | $\ln\theta_t = \ln\theta_0 - k_1 t$ | $\ln\theta_t$ $vs$ $t$ | $k_1$ = Slope; $\theta_0 = \exp$(Intercept) | [17] |
| 2 | Hill second-order Kinetics | $1/\theta_t = 1/\theta_0 - k_2 t$ | $1/\theta_t$ $vs$ $t$ | $\theta_0 = 1/$Intercept | [18] |
| 3 | Pseudo second-order Kinetics | $t/\theta_t = 1/(k_2\theta_0^2) + t/\theta_0$ | $t/\theta_t$ $vs$ $t$ | $\theta_0 = 1/$Slope | [11] |
| 4 | Intra-particle Diffusion | $\theta = K_d t^{1/2} + C$ | $\theta$ $vs$ $t^{1/2}$ | $K_d$ = Slope; $C$ = Intercept | [19] |

### 2.4.1 Oil sorption capacity

The sorption of oil from water was carried out using the methods of Banerjee et al. (2006) [20]. To simulate the situation of oil spill and minimize experimental variation, the crude oil sample

was held in beakers for one day in open air to release volatile hydrocarbon contents. The raw and acetylated samples were then subjected to crude oil sorption test. To 100mL of distilled water in a 250mL beaker, 5 g of crude oil was added. A portion (1 g) of the sorbent was added into the mixture in the beaker. The mixture was allowed to stand for about 3 minutes with little agitation. The sorbents were removed from the beakers using a sieve net and left to drain by hanging the net over the beaker in an oven for 30 minutes at $60^oC$ and weighed. The same procedure was repeated for the other four samples. The oil sorption capacity was calculated by taking into account the weight of sorbent, weight of sorbent and oil and weight of sieve net.

$$\mathrm{Oilsorptioncapacity(g/g)} = \frac{\mathrm{S_{st} - S_o}}{\mathrm{S_o}} \tag{3}$$

Where $S_o$ is the initial mass of the dry sorbent, $S_{st}$ is the mass of the sorbent with oil at the end of the sorption test and the ($S_{st}$ – $S_o$) quantity is the net oil sorbed (all of the masses were measured in grams). The amount of crude oil adsorbed ($q_e$) in milligrams per gram was determined using the following mass balance equation:

$$\mathrm{q_e} = \frac{(\mathrm{C_o} - \mathrm{C_e})\mathrm{V}}{\mathrm{m}} \tag{4}$$

Where, $C_o$ is the initial oil concentration in mg/L, $C_e$ is the equilibrium oil concentration in mg/L, V is the solution in liters, and *m* is the mass of the adsorbent in g.

Key: $C_e$ is the equilibrium concentration of the adsorbate (mg/L), $q_e$ and $q_m$ are equilibrium and maximum monolayer adsorption capacities (mg/g), respectively. KL is the Langmuir constant (L/mg) and B are Temkin constants, and $K_F$ $[(mg/g)(L/g)^{1/n}$ and n are Freundlich constants related to adsorption capacity and intensity, respectively.

## 2.5 Statistical Analysis

Comparative adsorption between modified and unmodified samples was analyzed using two-way ANOVA test at a 95% confidence interval in excel version of 2010 p-values less than the 0.05 significance level showed significant variations in the mean values of oil sorption capacity.

# 3 Results and Discussion

## 3.1 Scanning electron microscopy (SEM) analysis

Figure 2a and Figure 2b sample revealed a surface texture and porosity. The SEM was determined to verify the presence of macro-pores in the structure of the sample. The morphology of the raw and acetylated *Luffa aegyptiaca* sponge are presented in Figure 2a and Figure 2b, respectively. Figure 2a shows a scanning electronic micrograph of the raw sample at 1500x. It shows the surface of the morphologies and cross section of the sample observed in Figure 2a and Figure 2b. The raw sample of *Luffa aegyptiaca* sponge has a unique structural composition. Its shape is elongated, fibrous, spongy as the name implies and porous. The results presented in Figure 2a and Figure 2b shows a rectangular cell shape with large intercellular spaces. These provide the adsorption support required. 2a shows the surface morphology of raw *Luffa aegyptiaca* sponge taken at 1500x magnification, the image exhibits a rough and uneven surface, suggesting the presence of micro-pores and macro-pores, which could be beneficial for applications requiring high surface area, such as adsorption. The interconnected porous structure suggests high porosity, which enhances fluid adsorption and permeability. This aids in efficient mass transfer for adsorption. The surface shows undulating and interwoven structures, likely corresponding to the natural fibrous network of *Luffa aegyptiaca* sponge. The fibrous, interwoven micro-structure contributes to structural integrity while maintaining flexibility. The morphology could influence mechanical properties like flexibility and compressibility. The presence of ridges, depressions and voids indicates a naturally occurring structure, which is typical for plant-based biomaterials. In Figure 2b the morphology was taken at 500x. When compared to the raw *Luffa aegyptiaca* sponge, it exhibits notable changes in the structure due to acetylation. The acetylated process changed the configuration of the sample; this became loose, irregular and flaky structures. The presence of granular or aggregated formations suggests that the modification introduced surface roughening and potential deposition of the reaction of byproducts. It also showed that the surface of the acetylated sample was more ruptured along with different degrees of wrinkles which increased the surface area. Unlike the raw *Luffa aegyptiaca* sponge which has a more interconnected fibrous morphology, the data in Figure 2b

seems to have lost some of its structural integrity, due to the chemical alteration of cellulose and hemicellulose [21]. The acetylation process likely introduced swelling or disruption of the natural fiber arrangement. The smoother regions interspersed with flaky deposits suggests the presence of a newly formed layer, possibly an acetyl group modifying the cellulose structure. From the data presented in Figure 2b, the acetylation process typically enhanced the water resistance, making the material more suitable for oil absorption. The new rough and fragmented surface may provide sites for further functionalization, enabling applications in catalysis or composite materials [22].

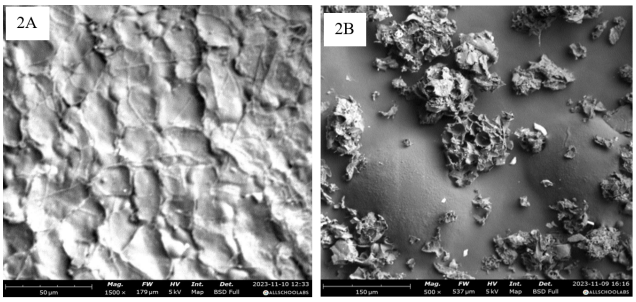


**Figure 2** (a) SEM micrograph image at mag.1500 x for raw; (b) SEM micrograph image at mag.500 x for acetylated *Luffa aegyptiaca* sponge

## 3.2 FTIR Analysis

The FTIR spectra of both raw and acetylated *Luffa aegyptiaca* sponge sample in the range 3553.31 to 506 $cm^{-1}$ are shown in Figure 3a and Figure 3b. The peaks observed at 350.71,3374.32, 3312.31, 3281.57, 2923.38, 2852.38 1633.66, 1534.37, 1397.71, 1241.21, 1032.18, 616.19, 596.32, 569.56, 561.36, 55.96, 530.04 and 508.22$cm^{-1}$ are associated with the raw *Luffa aegyptiaca* sponge while those observed at 3283.05, 2926.00, 2219.27, 2192.56, 2160.52, 2039.37, 1617.97, 1509.46, 1420.15, 1316.52, 1228.08, 1029.04, 606.48, 573.44, 560.43, 526.65 and 512.81$cm^{-1}$ in the spectra of the acetylated *Luffa aegyptiaca* sponge provide some evidence of acetylation [9]. The acetylated *Luffa aegyptiaca* sponge spectrum at 3283.05$cm^{1}$ shows hydroxyl stretching and N-H stretching vibration region. The absorption indicates significant presence of hydroxyl or amine groups. The broad peak indicates hydrogen bonding or molecular interactions. The hydroxyl (O-H) stretching is located in the alcohols (3250-3600 $cm^{-1}$), Phenols (3300-3500 $cm^{-1}$ and carbohydrates (3200-3600$cm^{-1}$). The amines (N-H) stretching in primary amines (3300-3500 $cm^{-1}$ and secondary amines (3200-3400 $cm^{-1}$) with the possible functional groups as Primary amines (-$NH_2$), Secondary amines (-NHR), Imides (-NH-C=O) and amines (-$NH_2$, -NHR). N-H stretching often appears as a doublet or broad band. The presence of N-H bands may indicate multiple amine groups and different amine environments. The raw sample at 3503.71$cm^{-1}$ typically corresponds to a specific molecular vibration. It is assigned to O-H stretching vibration. The possible functional group present are hydroxyl (-OH) group, likely from alcohols (primary, secondary or tertiary), phenols, carboxylic acid (as a broad, weaker band) and Hydrogen bonded O-H (weaker intensity). The position of the band suggests a relatively strong, free OH stretching vibration. At 3374.32$cm^{-1}$ and 3312.31$cm^{-1}$ the wave numbers typically correspond to N-H stretching vibration (primary or secondary amine) [23]. The possible functional groups are primary amines (-$NH_2$, secondary amines (-NHR), amides) -NHC=O) and Imides (-NH-C=O). The position and intensity suggest a relatively strong, free N-H stretching vibration. The band shape can indicate hydrogen bonding (broadening or shifting) and narrowing or splitting. At 2923.38 and 2926.00$cm^{-1}$ the wave numbers are assigned to C-H stretching vibration. The possible functional groups are alkenes, alkyl chains and cycloalkanes [24]. The position indicates a relatively strong free C-H stretching vibration, the band shape and width suggest a moderate molecular interaction (Van dar Waals). These peaks suggest a complex molecule with hydrogen bonding, molecular interactions and multiple functional groups. At 2219.27, 2192.56, 2160.52 and 2039.37$cm^{-1}$ typically corresponds to C≡ N stretching vibration (nitrile group). The possible functional groups assigned the wave numbers nitriles (-C≡ N), Isocyanides (-C≡ N-R) and Cyanates (-O-C≡ N). Its position indicates a relatively strong free C≡ N stretching vibration. The band shape and width suggest moderate molecular interactions. Some possible molecular structures associated with these peaks are alkynes, Isocyanides, Polymers with alkyne or isocyanide groups and biological molecules. At 1633.66 and 1617.97 cm is assigned to C=C stretching vibration (alkene) or C=O stretching vibration (amide, ketone or aldehyde). Its position indicates a

relatively strong free C=C or C=O stretching vibration. The band shape and width suggest moderate molecular interactions. At 1534.37 and 1509.46cm$^{-1}$ is assigned to N-H bending vibration (amide II) or C=C stretching vibration (aromatic) [25]. The possible functional groups are amides (-N-C=O, amide II), aromatic compounds (C=C, benzene ring), heterocycles (C=N, C=C) and Imides (-N-C=O). Its position indicates a relatively strong, free N-H bending or C=C stretching vibration. The band shape and width suggest moderate molecular interactions (hydrogen bonding). 1397.71cm$^{-1}$ is assigned to C-N stretching vibration (Aliphatic amines), C-O stretching vibration (alcohols, ethers) and $CH_3$ bending vibration (symmetric). Possible functional groups associated are aliphatic amines (-C-N), alcohols (-C-OH), esters (-C-O-C) and methyl groups (-$CH_3$). The spectrum at 1420.15 cm$^{-1}$ shows $CH_2$ bending, $CH_3$ bending vibration, C-N stretching vibration (aromatic amines), and C-O stretching vibration. Its position indicates a relatively strong free $CH_2$or $CH_3$ bending vibration [26, 27]. The results showed that the acetylated sample had an appreciable result which could make wastes from the sample an industrial raw material. The degree of substitution increases with time. The sample could be a good substitute for adsorption in industrial products where acetylation is applicable. The disappearance or shifting of the-OH stretch (O-H stretching region) suggests that hydroxyl (-OH) groups were replaced by acetyl groups (successful acetylation). Slight shifts in the C–H stretch (C-H stretch region (Alkenes)) bands suggest minor structural changes due to acetylation [28]. The presence of a C=O stretch in the acetylated sample confirms the formation of acetyl ester or ketone groups. The minor shifts and changes in peak intensity suggest some alterations in the aromatic or C=C structures. The increase in C-O stretching peaks indicates an ester formation. Small shifts in the low frequency region (skeletal vibrations, bending) indicate changes in the molecular skeleton [29]. (see Figure 3)

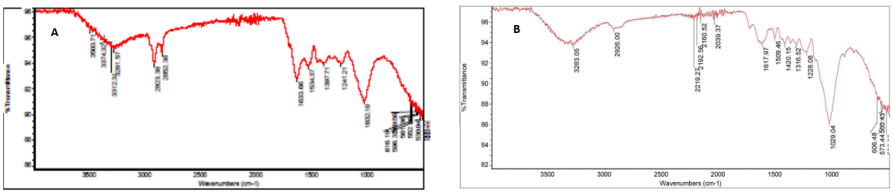


**Figure 3** (A) Spectra of raw; (B) acetylated *Luffa aegyptiaca* sponge

## 3.3 Adsorption Tests

### 3.3.1 Effect of time on crude oil sorption onto *Luffa aegyptiaca* sponge

The analysis of crude oil by Luffa *aegyptiaca* sponge was studied and the results were presented in Figure 4.

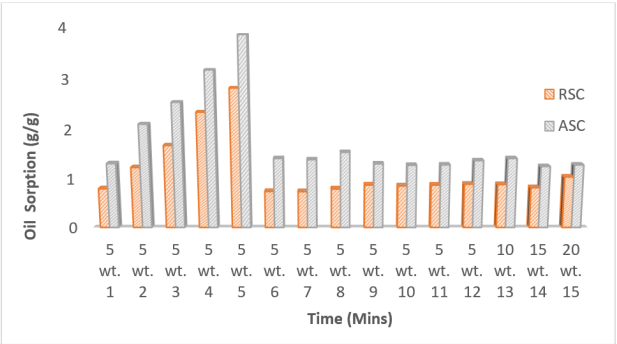


**Figure 4** Effect of contact time on oil sorption capacity of raw and acetylated *Luffa aegyptiaca* sponge

The oil sorption capacity of both the Raw Sample C (RSC) and Acetylated Sample C (ASC) increase initially with contact time. The maximum oil sorption capacity for both samples is achieved at around 5 minutes. The oil sorption capacity of both RSC and ASC increases rapidly during the initial stages of contact. This can be attributes to the availability of active sorption sites on the surface of the samples, which facilitates the adsorption of oil [30]. After reaching a peak at around 5 minutes, the oil sorption capacity of both samples gradually decreases and then levels off. This indicates that the sorption sites become saturated, and the samples reach an equilibrium state where the rate of oil adsorption equals the rate of oil desorption. ASC exhibits

a higher maximum oil sorption capacity compared to RSC, as evident from the graph. The rate of oil sorption of ASC appears to be faster than the RSC, as indicated by the steeper increase in oil sorption capacity during the initial stages of contact.

## 3.4 Equilibrium Studies

### 3.4.1 Adsorption Isotherm model studies

Adsorption equilibrium studied was done using adsorption isotherms to determine the surface properties of the adsorbents. The Freundlich, Langmuir and Temkin isotherms, as expressed in Table 1 and presented in Figure 4a-4f. Results of the sorption isotherm for Freundlich model of adsorption of acetylated *Luffa aegyptiaca* sponge. (see Table 3)

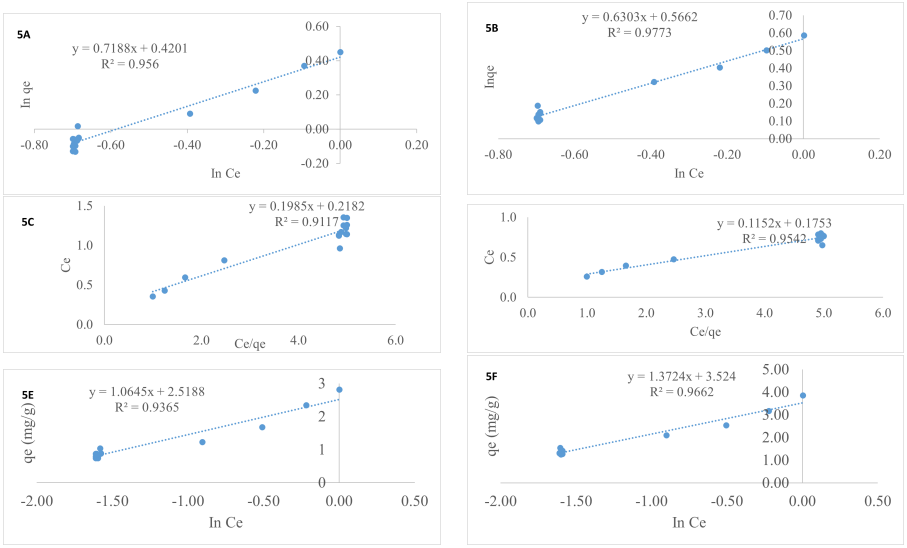


**Figure 5** (A) Freundlich model (raw); (B) Freundlich model (acetylated); (C) Langmuir model (raw); (D) Langmuir model (acetylated); (E) Temkin model (raw); (F) Temkin model (acetylated) of crude oil adsorption for *Luffa aegyptiaca* sponge.

**Table 3** Isotherm parameters for crude oil adsorption on *Luffa aegyptiaca* sponge

| Isotherm model | RSC | ASC |
|---|---|---|
| Freundlich model | | |
| Intercept (log $K_F$) | 0.4291 | 0.5662 |
| n (g/L) | 1.391 | 1.587 |
| $K_F$(g/g)(L/g)$^{1/n}$ | 1.54 | 3.67 |
| $R^2$ | 0.9560 | 0.9773 |
| Langmuir model | | |
| $Q_0$ (1/slope) g/g) | 5.0378 | 8.6810 |
| 1/$Q_0$(slope) | 0.1985 | 0.1152 |
| Intercept (1/$Q_0$B) | 0.2182 | 0.1753 |
| B(L/mg)(1/$Q_0$ x intercept) | | 0.656 |
| $R^2$ | 0.9117 | 0.9542 |
| Temkin model | | |
| Intercept | 2.5188 | 3.524 |
| Slope | 1.0645 | 1.3724 |
| $R^2$ | 0.9365 | 0.9662 |
| b (Temkin Constant at 30$^o$C) | 1.0645 J/mol | 1.3724 J/mol |
| $K_T$(Temkin Binding constant at 30$^o$C) | 10.66 L/g | 13.04 L/g |

Figure 5a represents the Freundlich model of adsorption for acetylated *Luffa aegyptiaca* sponge. The value of 1/n is 0.6303 is between 0 and 1 indicating favourable adsorption. The $R^2$ value is 0.9773 with a high correlation coefficient which suggests that the Freundlich isotherm model very well describes the adsorption behaviour of the acetylated *Luffa aegyptiaca* sponge. The higher intercept ($K_F$) (0.5662) suggests strong adsorption capacity due to acetylation, which likely increased surface functionality. The Freundlich adsorption capacity ($K_F$) is 0.5662. The $R^2$ value which is close to 1 suggests that the Freundlich model describes the adsorption process better. This confirms that the adsorption follows multilayer coverage on a

heterogeneous surface rather than the monolayer adsorption. The value of 1/n 0.6303 suggests a moderately strong adsorption. If 1/n $<$ 1, it signifies that adsorption is favourable, which aligns with the trend in Figure 5a. The adsorption of the acetylated *Luffa aegyptiaca* sponge on the adsorbent follows the Freundlich isotherm model better, as indicated by the high $R^2$ value. The results suggest a heterogeneous adsorption process where the adsorbent surface has sites with varying affinities for the adsorbate. This also implies that as concentration increases, adsorption efficiency decreases, aligning with the characteristics of the Freundlich model. In Figure 5b, represents the Langmuir isotherm model for adsorption, where the ratio of equilibrium concertation to the amount adsorbed ($C_e/q_e$) was plotted against the equilibrium concentration (Ce). From the equation for Langmuir isotherm model the linear regression has a high correlation coefficient (0.9542), indicating a good fit for the Langmuir model. The slope ($1/q_{max}$) gives 0.1152, the inverse of this gives the maximum adsorption capacity($q_{max}$), which represents the highest amount of adsorbent can hold. With the intercept $1/q_{max}K_1$ is 0.1753 the Langmuir constant ($K_L$), is determined [11, 31]. From the results presented above. The $R^2$ value 0.9542 suggests that the data fits the Langmuir isotherm model reasonably well but not perfectly as the Freundlich isotherm model by comparing the $R^2$ value for the raw and acetylated results above for Langmuir model $R^2$ or the raw sample gave 0.9773 (better fit) and $R^2$ value for the acetylated sample gave 0.9542 (weaker fit). The Temkin isotherm model assumes that the adsorption energy of molecules decreases linearly with surface coverage due to interactions between adsorbate and adsorbent. Figure 5e and 5f represents the Temkin adsorption isotherm for raw and acetylated *Luffa aegyptiaca* sponge representing a linearized Temkin isotherm with the slope of 1.0645 / 1.3724 and intercept 2.5188 / 3.524 respectively. The acetylated sponge has an $R^2$ of 0.9662, which is higher than the raw sample. This indicates a better fit of the Temkin model to the adsorption process for the acetylated sample. The acetylated sample has a higher b (13724) compared to the raw sample (1.0645). This suggests that the heat of adsorption (b) is lower for the acetylated sample, indicating a more uniform adsorption energy distribution [32]. The acetylated sample has a higher intercept (3.524 against 2.5188), indicating the equilibrium binding constant $K_T$ is also higher (13.04 against 10.66). However, the acetylation process improved the adsorption performance as shown by the higher $R^2$, b, and $K_T$ values suggesting that acetylation enhances the surface properties, making the sample a better adsorbent. But the Freundlich isotherm model has a better correlation, by implying that adsorption from acetylated is heterogeneous and multi-layered rather than homogeneous and mono-layered. The Langmuir and Temkin isotherm models are less suitable for this adsorption process. Thus, acetylation proved a beneficial modification for improving the adsorption capacity of *Luffa aegyptiaca* sponge.

## 3.5 Kinetic Studies

### 3.5.1 Kinetic studies of crude oil sorption on *Luffa aegyptiaca* sponge

Figure 6a represents the first order kinetic model for sorption of oil on raw *Luffa aegyptiaca* sponge. The $R^2$ value is 0.0169, indicating a very poor fit of the first order model to the experimental data. This suggests that the sorption process does not follow a first order model to the data. This suggests that the sorption process does not follow first-order kinetics. The low $K_1$ value (0.012) suggests a slow sorption rate, implying that equilibrium takes a long time to be reached. Figure 6b shows the first order kinetic model for sorption of oil on acetylated *Luffa aegyptiaca* sponge. The rate constant $K_1$ is 0.0247 this is higher than that of the raw sample. This suggests that acetylation treatment improved the sorption kinetics, possibly due to enhanced surface properties or better interaction with oil molecules. The calculated qe (1.954), which is higher than that of raw sample (1.142). This indicates that acetylation increases the oil sorption capacity, likely due to increased hydrophobicity. The $R^2$ value (0.0945) is very low, meaning the first-order model does not fit well. This low correlation suggests that other models might describe the kinetics more accurately. Figure 6c represents the Hill second order kinetic model for sorption of oil on raw *Luffa aegyptiaca* sponge. The $R^2$ value is very low, indicating that the second order model does not accurately describe the sorption kinetics of oil on the raw *Luffa aegyptiaca* sponge. This suggests that there are other kinetic models that might better explain the sorption process. The high calculated equilibrium adsorption capacity qe value indicates a relatively high adsorption capacity of the sponge for oil. However, due to the poor fit (low $R^2$), this value may not be reliable. The value of $K_2$ suggests that the adsorption process is slow under the given experimental conditions. This could be due to the limitations in available adsorption sites, or diffusion constraints. The second order kinetic model suggests a slow adsorption rate and a high theoretical adsorption capacity. However, the extremely low $R^2$ value indicates that this model does not effectively describe the actual sorption kinetics. Figure 6d shows

the Hill second order kinetic model for sorption of oil on acetylated *Luffa aegyptiaca* sponge when compared with the raw sample the higher adsorption capacity (which had a higher qe), this lower value suggests that acetylation might have altered the material's surface properties, possibly reducing the active sites for oil sorption. The calculated $K_2$ indicates that the sorption rate is faster than that of the raw sample. This suggests that surface modification might have improved the reaction kinetics by increasing the availability of active sites or enhancing the interaction between the oil and the sorbent. The low $R^2$ value suggests that the second order model does not fit the experimental data well. Figure 6e shows the Pseudo second order kinetic model for sorption of oil on raw *Luffa aegyptiaca* sponge. The linear behaviour suggests that the adsorption follows a pseudo-second order kinetic model, implying that the rate of sorption depends on the square of the number of available adsorption sites. The positive slope confirms that adsorption increases with time. The coefficient of determination of the data from Figure 6f ($R^2$-0.9512) suggests a very strong correlation, indicating that the model effectively describes the adsorption process. The increased $R^2$ value when compared to the data from the raw *Luffa aegyptiaca* sponge, suggests that acetylation improves the fit of the kinetic model, likely due to chemical modifications enhancing the adsorption capacity. A lower slope was observed in the result above when compared with the data obtained from the raw *Luffa aegyptiaca* sponge, meaning it can hold more oil at equilibrium. The low value $R^2$ observed from figure. Figure 6g and 6h indicates a very poor correlation between the data. Suggesting that intra-particle diffusion is not fit for the rate controlling step in the sorption process. The high intercept value suggests that an external boundary layer resistance is significant. (see Table 4)

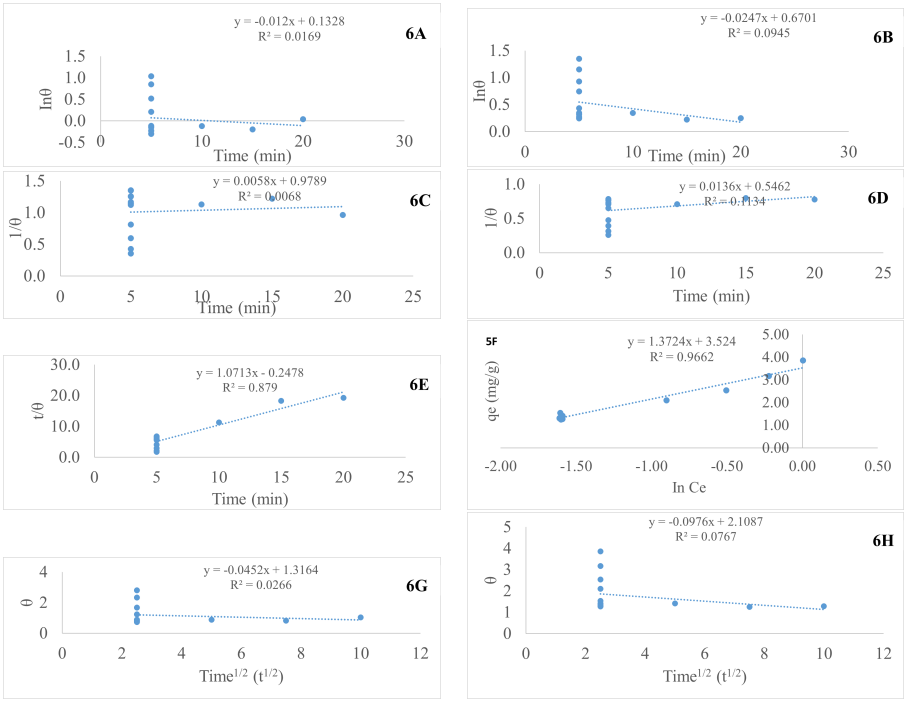


**Figure 6** (A) First order (raw); (B) First order (acetylated); (C) Second order (raw); (D) Second order (acetylated); (E) Pseudo-second order (raw); (F) Pseudo-second order (acetylated); (G) Intra-particle diffusion; (H) Intra-particle diffusion (acetylated). Kinetic model(s) for crude oil sorption of *Luffa aegyptiaca* sponge

# 4 Conclusion

The raw *Luffa aegyptiaca* sponge has highly porous, fibrous and spongy structure. It shows interconnected micro- and macro –pores which is beneficial for adsorption applications. The natural structure includes ridges, depressions, and voids, typical of plant-based biomaterials. The acetylation process significantly alters the morphology of the sponge. Acetylated samples show higher surface area and roughness. Acetylated sponge loses some structural integrity due to chemical alterations of cellulose and hemicellulose. The observed changes are favourable for adsorption despite structural weakening. New absorption bands in the acetylated sample spectrum provide clear evidence of chemical modification through acetylation these changes indicate the introduction of new functional groups and alteration of existing ones. Both raw and

**Table 4** Kinetic parameters for crude oil sorption on *Luffa aegyptiaca* sponge

| Type | Raw sample *Luffa aegyptiaca* sponge | Acetylated Sample *Luffa aegyptiaca* sponge |
|---|---|---|
| First order kinetics | | |
| Intercept (C) | 0.1328 | 0.6701 |
| qe calc (mg/g) | 1.142 | 1.954 |
| $R^2$ | 0.0169 | 0.0945 |
| (Slope) K1 ($min^{-1}$) | 0.012 | 0.0247 |
| Second order kinetics | | |
| Intercept | 0.9789 | 0.5462 |
| qe calc mg/g | 172.41 | 73.53 |
| $R^2$ | 0.0068 | 0.1134 |
| (Slope) | 0.0058 | 0.0136 |
| $K_2$ | $3.44 \times 10^{-5}$ | 3.39 |
| Pseudo second order kinetics | | |
| Intercept | -0.2478 | 1.186 |
| qe calc mg/L | 0.9335 | 1.178 |
| $R^2$ | 0.879 | 0.9512 |
| (slope) | 1.0713 | 0.8488 |
| $K^2$ | 4.56 | 0.606 |
| Intra-particle Diffusion | | |
| Kd (slope) | -0.0452 | -0.0976 |
| C(intercept) | 1.3164 | 2.1087 |
| $R^2$ | 0.0266 | 0.0767 |

acetylated samples showed bands corresponding to hydroxyl (OH) and amine (NH) stretching vibrations. Hydroxyl (-OH), alcohols (primary, secondary, tertiary), phenols, carboxylic acids, and hydrogen-bonded -OH. Primary amines (-$NH_2$), secondary amines (-NHR), amides and imides. There is evidence of structural changes in the acetylated samples: band shifts and new peaks indicate changes in C-H stretching vibrations, suggesting alkylation or addition of acetyl groups. Changes in band intensity and position point to altered hydrogen bonding, increased molecular interaction, and possible van der Waals forces. Furthermore, the presence of broader, split, or doublet bands suggests a complex molecular environment with multiple hydrogen-bonding interactions within the modified sponge structure. The adsorption process appears to be heterogeneous, suggesting that the adsorbent surface has sites with varying affinities for the adsorbate. This supported by the better fit of the Freundlich isotherm model. The acetylation enhances the adsorption capabilities of the sample. Making it a better adsorbent. This is indicated by the improved $R^2$, b, and KT values.

The acetylated sample shows a more uniform adsorption energy distribution and a higher equilibrium binding constant suggesting improved adsorption performance. Statistical analysis ANOVA revealed a strong significant relation between the variables provided.

# Author Contributions

**Adaku Chinonyerem Ajiwe:** Writing – original draft, review and editing, Methodology, Data curation, Conceptualization, Software, Formal analysis,

**Patrice-Anthony Chudi Okoye:** Writing – review & editing.

**Uche Eunice Ekpunobi:** Writing – review & editing, Resources.

# Data Availability Statement

All data analyzed in this study can be found in the tables and figures presented above.

# Conflicts of Interest

The authors declare that they have no known conflicting financial interests or personal relationships that could have appeared to influence the work reported in this paper.

# References


[1] Asadpour, R., Sapari, N. B., Isa, M. H., Kakooei, S., & Orji, K. U. (2015). Acetylation of corn silk and its application for oil sorption. Fibers and Polymers, 16(9), 1830-1835. https://doi.org/10.1007/s12221-015-4745-8

[2] Asadpour R, Sapari NB, Isa MH, et al. Acetylation of corn silk and its application for oil sorption. Fibers and Polymers. 2015, 16(9): 1830-1835. https://doi.org/10.1007/s12221-015-4745-8

[3] Alaa El-Din G, Amer AA, Malsh G, et al. Study on the use of banana peels for oil spill removal. Alexandria Engineering Journal. 2018, 57(3): 2061-2068. https://doi.org/10.1016/j.aej.2017.05.020

[4] Sun X. Acetylation of sugarcane bagasse using NBS as a catalyst under mild reaction conditions for the production of oil sorption-active materials. Bioresource Technology. 2004, 95(3): 343-350. https://doi.org/10.1016/j.biortech.2004.02.025

[5] Abdelwahab O, Nasr SM, Thabet WM. Palm fibers and modified palm fibers adsorbents for different oils. Alexandria Engineering Journal. 2017, 56(4): 749-755. https://doi.org/10.1016/j.aej.2016.11.020

[6] Husin, N. I., Wahab, N. A. A., Isa, N., & Boudville, R. (2011, June). Sorption equilibrium and kinetics of oil from aqueous solution using banana pseudostem fibers. In International conference on environment and industrial innovation (Vol. 12, pp. 177-182).

[7] Wang, J., Zheng, Y., & Wang, A. (2012). Effect of kapok fiber treated with various solvents on oil absorbency. Industrial crops and products, 40, 178-184. https://doi.org/10.1016/j.indcrop.2012.03.002

[8] Olga, V. R., Darina, V. I., Alexandr, A. I., & Alexandra, A. O. (2014). Cleanup of water surface from oil spills using natural sorbent materials. Procedia Chemistry, 10, 145-150.

[9] Wang J, Zheng Y, Wang A. Effect of kapok fiber treated with various solvents on oil absorbency. Industrial Crops and Products. 2012, 40: 178-184. https://doi.org/10.1016/j.indcrop.2012.03.002

[10] Olga VR, Darina VI, Alexandr AI, et al. Cleanup of Water Surface from Oil Spills Using Natural Sorbent Materials. Procedia Chemistry. 2014, 10: 145-150. https://doi.org/10.1016/j.proche.2014.10.025

[11] Adebajo MO, Frost RL. Acetylation of raw cotton for oil spill cleanup application: an FTIR and 13C MAS NMR spectroscopic investigation. Spectrochimica Acta Part A: Molecular and Biomolecular Spectroscopy. 2004, 60(10): 2315-2321. https://doi.org/10.1016/j.saa.2003.12.005

[12] American Standards for testing and Materials (ASTM), (F726-99). (1998). Standard Test Method for Sorbent Performance of Adsorbents. Annual Book of ASTM standards ASTM Committee on Standards. West Conshohocken, PA 1201-1206.

[13] Ismail, A. S. (2015). Preparation and evaluation of fatty-sawdust as a natural biopolymer for oil spill sorption. Chemistry Journal, 5(5), 80-85.

[14] Nwadiogbu JO, Ajiwe VIE, Okoye PAC. Removal of crude oil from aqueous medium by sorption on hydrophobic corncobs: Equilibrium and kinetic studies. Journal of Taibah University for Science. 2016, 10(1): 56-63. https://doi.org/10.1016/j.jtusci.2015.03.014

[15] Rahangdale, D., & Kumar, A. (2018). Chitosan as a substrate for simultaneous surface imprinting of salicylic acid and cadmium. Carbohydrate polymers, 202, 334-344. https://doi.org/10.1016/j.carbpol.2018.08.129

[16] Mahmoud, M. A. (2020). Oil spill cleanup by raw flax fiber: Modification effect, sorption isotherm, kinetics and thermodynamics. Arabian Journal of Chemistry, 13(6), 5553-5563. https://doi.org/10.1016/j.arabjc.2020.02.014

[17] Diraki A, Mackey H, McKay G, et al. Removal of oil from oil–water emulsions using thermally reduced graphene and graphene nanoplatelets. Chemical Engineering Research and Design. 2018, 137: 47-59. https://doi.org/10.1016/j.cherd.2018.03.030

[18] Rahangdale D, Kumar A. Chitosan as a substrate for simultaneous surface imprinting of salicylic acid and cadmium. Carbohydrate Polymers. 2018, 202: 334-344. https://doi.org/10.1016/j.carbpol.2018.08.129

[19] Mahmoud MA. Oil spill cleanup by raw flax fiber: Modification effect, sorption isotherm, kinetics and thermodynamics. Arabian Journal of Chemistry. 2020, 13(6): 5553-5563. https://doi.org/10.1016/j.arabjc.2020.02.014

[20] Shin HS, Kim JH. Isotherm, kinetic and thermodynamic characteristics of adsorption of paclitaxel onto Diaion HP-20. Process Biochemistry. 2016, 51(7): 917-924. https://doi.org/10.1016/j.procbio.2016.03.013

[21] Oloo CM, Onyari JM, Wanyonyi WC, et al. Adsorptive removal of hazardous crystal violet dye form aqueous solution using Rhizophora mucronata stem-barks: Equilibrium and kinetics studies. Environmental Chemistry and Ecotoxicology. 2020, 2: 64-72. https://doi.org/10.1016/j.enceco.2020.05.001

[22] Dawodu MO, Akpomie KG. Evaluating the potential of a Nigerian soil as an adsorbent for tartrazine dye: Isotherm, kinetic and thermodynamic studies. Alexandria Engineering Journal. 2016, 55(4): 3211-3218.
https://doi.org/10.1016/j.aej.2016.08.008

[23] Banerjee SS, Joshi MV, Jayaram RV. Treatment of oil spills using organo-fly ash. Desalination. 2006, 195(1-3): 32-39.
https://doi.org/10.1016/j.desal.2005.10.038

[24] Wahi R, Chuah LA, Choong TSY, et al. Oil removal from aqueous state by natural fibrous sorbent: An overview. Separation and Purification Technology. 2013, 113: 51-63.
https://doi.org/10.1016/j.seppur.2013.04.015

[25] Onwuka JC, Agbaji EB, Ajibola VO, et al. Kinetic studies of surface modification of lignocellulosic Delonix regia pods as sorbent for crude oil spill in water. Journal of Applied Research and Technology. 2016, 14(6): 415-424.
https://doi.org/10.1016/j.jart.2016.09.004

[26] Oliveira LMTM, Oliveira LFAM, Sonsin AF, et al. Ultrafast diesel oil spill removal by fibers from silk-cotton tree: Characterization and sorption potential evaluation. Journal of Cleaner Production. 2020, 263: 121448.
https://doi.org/10.1016/j.jclepro.2020.121448

[27] Nnaji NJN, Okoye COB, Obi-Egbedi NO, et al. Spectroscopic Characterization of Red Onion Skin Tannin and It's use as Alternative Aluminium Corrosion Inhibitor in Hydrochloric Acid Solutions. International Journal of Electrochemical Science. 2013, 8(2): 1735-1758.
https://doi.org/10.1016/s1452-3981(23)14261-1

[28] Wekoye JN, Wanyonyi WC, Wangila PT, et al. Kinetic and equilibrium studies of Congo red dye adsorption on cabbage waste powder. Environmental Chemistry and Ecotoxicology. 2020, 2: 24-31.
https://doi.org/10.1016/j.enceco.2020.01.004

[29] Birhanu Y, Leta S, Adam G. Removal of chromium from synthetic wastewater by adsorption onto Ethiopian low-cost Odaracha adsorbent. Applied Water Science. 2020, 10(11).
https://doi.org/10.1007/s13201-020-01310-3

[30] Onwu DO, Ogbodo ON, Ogbodo NC, et al. Application of Esterified Ogbono Shell Activated Biomass as an Effective Adsorbent in the Removal of Crude Oil layer from Polluting Water Surface. Journal of Applied Sciences and Environmental Management. 2019, 23(9): 1739.
https://doi.org/10.4314/jasem.v23i9.20

[31] Choudhury, T. R., Rahman, M. S., Liba, S. I., Islam, A., Quraishi, S. B., Begum, B. A., ... & Amin, M. N. (2022). Adsorptive removal of chromium from aqueous solutions using flax (Linum usitatissimum): Kinetics and equilibrium studies. Environmental Chemistry and Ecotoxicology, 4, 132-139.
https://doi.org/10.1016/j.enceco.2022.02.004

[32] Purwaningrum, W., Vilantina, V., Rizki, W. T., Desnelli, D., Hariani, P. L., & Said, M. (2021). Cr (III)-doped bentonite: synthesis, characterization and application for phenol removal. Makara Journal of Science, 25(2), 2.
https://doi.org/10.7454/mss

[33] Hoang AT, Le VV, Al-Tawaha ARMS, et al. An absorption capacity investigation of new absorbent based on polyurethane foams and rice straw for oil spill cleanup. Petroleum Science and Technology. 2018, 36(5): 361-370.
https://doi.org/10.1080/10916466.2018.1425722

[34] Choudhury TR, Rahman MS, Liba SI, et al. Adsorptive removal of chromium from aqueous solutions using flax (Linum usitatissimum): Kinetics and equilibrium studies. Environmental Chemistry and Ecotoxicology. 2022, 4: 132-139.
https://doi.org/10.1016/j.enceco.2022.02.004

[35] Dawodu FA, Akpomie KG. Simultaneous adsorption of Ni(II) and Mn(II) ions from aqueous solution unto a Nigerian kaolinite clay. Journal of Materials Research and Technology. 2014, 3(2): 129-141.
https://doi.org/10.1016/j.jmrt.2014.03.002